JOTCS A
Journal of the Turkish Chemical Society
Section: A
Chemistry
TURKISH CHEMICAL SOCIETY

Synthesis, Characteristics and Applications of Graphene Composites: A Survey

Biswajit Patra[1], Niharika Das[1], Ruturaj Sahoo[1], Dipak Kumar Sahoo[1], Biswajit Dalai[2*] Chhatrapati Parida[3] and Sarat Kumar Dash[4]**

[1] Department of Physics, School of Sciences, GIET University, Gunupur, 765022, India.
[2] Department of Physics, School of Sciences, GIET University, Gunupur, 765022, India.
[3] Department of Physics, Odisha University of Agriculture and Technology, Bhubaneswar, 751003, India.
[4] Department of Physics, Regional Institute of Education (NCERT), Bhubaneswar, 751022, India.

Abstract: Graphene is the name for a monolayer sheet of carbon atoms that are bonded together in a repeating pattern of hexagons. This sheet is only one atom thick. Monolayers of graphene stacked on top of each other. In this article, we have compared the characterization results of graphene and graphene oxide along with synthesis via different methods. A sigma bond connects each atom in a graphene sheet to its three closest neighbours and each atom also contributes one electron to a conduction band that covers the entire graphene sheet. Graphene when oxidized is called graphene oxide (GO) and is mostly used in photoelectric, materialistic, catalyst and energy fields due to its thermal, electrical and mechanical characteristics. It is also used in the field of medical science, drug delivery and biomedical applications. Graphene have been improved due to import of 3D printing technology. In last few years, graphene has taken the attention of most material science researchers due to its various applications. Graphene based polymers and nanocomposites are widely used in sensors, optoelectronics, magneto transport, automotive, biosensors, electronics and aerospace fields.

Keywords: Graphene, XRD, Raman spectroscopy, Applications.

Submitted: January 14, 2023. **Accepted:** May 30, 2023.

Cite this: Patra B, Das N, Sahoo R, Sahoo DK, Dalai B, Parida C, Dash SK. Synthesis, Characteristics and Applications of Graphene Composites: A Survey. JOTCSA. 2023;10(3):757-72.

DOI: https://doi.org/10.18596/jotcsa.1234196

***Corresponding author's E-mail:** *biswajit@giet.edu , **skdash59@yahoo.com

1. INTRODUCTION

In continuation to our earlier review on perovskite materials (1) and extraction of thorium (2), we have reported here the various synthesis routes of graphene and graphene oxide with their characteristics and applications. Graphene is a hexagonal planner carbon ring which is derived from 3D massive covalent structured graphite. Graphene based materials exist in both 2D and 3D structures (3-6). A single layer of graphene (SLG) was obtained by Novoselov et. al. (3, 4). Graphene is a sp^2 bonded carbon structure where atoms densely packed in a honeycomb crystal lattice and a two-dimensional crystal. Graphite oxide is mostly used for producing expandable amount of graphene oxide (GO) and reduced graphene oxide. GO produces stable dispersion because of its negative charge and interacts with the functional groups of textiles. Wearable e-textiles are flexible, washable, and long-lasting. To coat textiles with graphene, vacuum filtering, brush coating, direct electrochemical technique and screen-printing methods are employed. Single layer graphene shows high mobility of electrons, high optical transparency, high mechanical strength, high thermal conductivity and high surface area (3-6). A mono layer graphene sheet and graphene membranes are shown in Fig. 1.

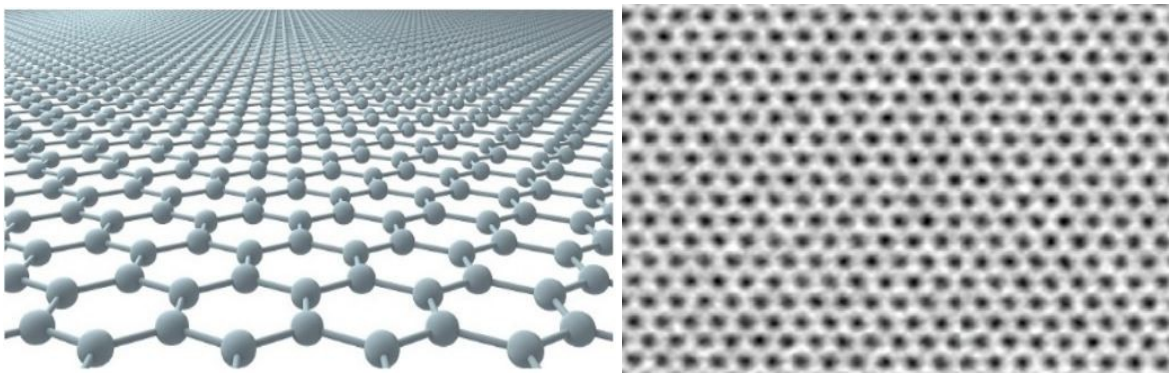

Figure 1: a. Mono layer graphene sheet **b.** Single layer graphene membranes.

Apart from these, graphene shows a countless advantage and it is a favourable for the evolution of recently invented applied science. Therefore, graphene is regarded as product material for high value applications such as sensor, water treatment, biomedical application, structural application (6-14). Graphene exhibits a whole range of electronic application due to its mechanical and other properties (14–17). Graphene based materials like GO & rGO are manufactured into wearable E-textiles which is safer for nature (16-22). Raman spectroscopy is used to find graphene optical phonons G-peak and 2D band (23-25). It is also used to count the number of atomic planes in few layers graphene (FLG) (25-27).

GO is formed by oxidizing graphene and it contains various oxygen-containing reactive groups such as carbonyl groups, epoxy groups, hydroxyl groups, and carboxylic groups (27, 28). The oxidation of bulk graphite powders using a chemical oxidation technique produces graphene oxide nanosheets (28-30). In 1859, Brodie had reported the developing work on production of GO (by adding a portion of potassium chloride to a slurry of graphite in fuming nitric acid) (30). The exact structure of GO is a difficult task to establish. GO and its products have been recently used in bio devices, biotechnology, bio sensors, energy storage and antifungal activity (28-31). GO is the forerunner of reduced graphene oxide (rGO).

2. EXPERIMENTAL SECTION

2.1. Synthesis of Graphene

2.1.1. Synthesis of graphene in top-down method

The top-down synthesis of graphene (Figure 2) includes the reduction of powered graphite. The commonly used synthesis processes are (i) mechanical exfoliation (ME), (ii) chemical exfoliation-reduction (CER), (iii) atomic force microscope (AFM) method, (iv) liquid phase exfoliation (LPE) method and (v) electrochemical exfoliation (ECE) method. Mechanical exfoliation method was developed by Novaselov et al. (3) SLG (single-layer graphite) with a lateral size of micrometer of highly oriented pyrolytic graphite, was physically peeled using household scotch tape in this procedure. As this process only produced small area of SLG, it was not suitable for large scale production (31–35). AFM method also produces FLG (1 to 6 layers) to MLG (multi-layer graphite: layers may vary up to 30 layers). Liquid phase exfoliation method includes two main steps: (i) a reduction reaction reduces Vander Waal stresses and increases graphite interlayer separation (33-35) and then (ii) Graphite exfoliated by rapid heating and sonication (or high shear forces) to yield graphene with single to several sheets (35, 36-39). An electric voltage is used in electrochemical exfoliation to force ionic species to interact and form graphite rods, where they create a gaseous molecule capable of exfoliating different graphene layers.

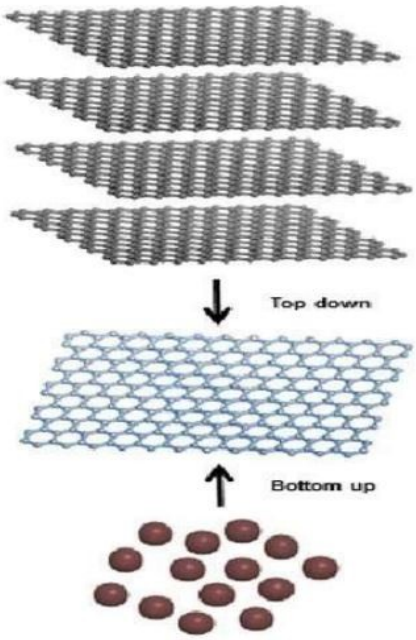

Figure 2: Synthesis of graphene by top down and bottom-up approach

Chemical oxidation reduction of graphite is the most standard method for synthesizing graphene (38-40). Graphite is first transformed to graphite oxide, which is then reduced to graphene by chemical, thermal, or electrochemical techniques. There are varieties of oxidation techniques: Staudenmaier's, Hummer's and Tour's methods (39-42). They oxidize graphite by adding concentrated acids and strong oxidants.

2.1.2. Synthesis of graphene by bottom-up method

This synthesis method (Figure 2) involves the use of hydrocarbon compounds as precursors (23, 24). Most commonly used bottom-up synthesis approaches are chemical vapour deposition (CVD), thermal pyrolysis, epitaxial growth, laser assisted synthesis and organic synthesis. CVD is a very

popular method of synthesizing carbon nanomaterial. Graphene is synthesized by the use of solid transition catalyst (41-43). It was produced in planer FLG films from camphor hydrolyzation, a Ni substrate using thermal CVD. Now we use this technique for production of a high-quality graphene. Further CVD modified including atmospheric CVD (APCVD) (23, 42–50). In this approach various carbon precursor from liquid and solid to gaseous molecules have been introduced to produce SLG to FLG. Precursors are: (i) gaseous: C_2H_2, C_2H_4, C_2H_6, C_3H_8 and (ii) liquid: C_6H_6, C_6H_{14}, C_2H_5OH, C_3H_7OH and (iii) solid: camphor source C_6Cl_6 multiwalled carbon nanotubes, fluorine, coronene (poly methyl methacrylate polystyrene and polycyclic aromatic hydrocarbon and waste plastic for preparation of graphene). There are numerous types of substrates including metals (copper, nickel, ferrum, gallium, silicon), alloys (CuNi and AuNi) oxides (Fe_2O_3, Al_2O_3, SiO_2 and MgO) stainless steel, mica germanium hexagonal boron nitrite and various glasses have been used for production of SLG to MLG using CVD. Mechanically exfoliated graphene produces similar graphene. The growth parameter influences the properties of CVD graphene, such as gas mass transfer, partial pressure, substrate selection, and carbon. Researchers are attempting to manage the amount of graphene layers, as well as the size, density, and flaws of grain boundaries and flaws.

2.1.3. Graphene synthesis in cleavage and exfoliation method

Many graphene sheets are piled together to form graphite, which is held together by a weak Vander wall force. Exfoliation and cleavage, which use mechanical or chemical energy to break these weak bonds and separate apart individual graphene sheets, can be used to generate graphene from a high purity graphite sheet. Exfoliation is the process of repeatedly peeling. Dry etching in oxygen plasma was used to create several 5 m deep mesas on a sheet of commercially available highly oriented pyrolytic graphite (HOPG) material. This was then applied to a photoresist, baked to adhere the mesas to the photoresist, released in acetone, and transferred to a Si substrate, where the graphene sheets were produced from a single to few layers thick. The scotch tape method of making graphene from HOPG is shown in Fig. 3.

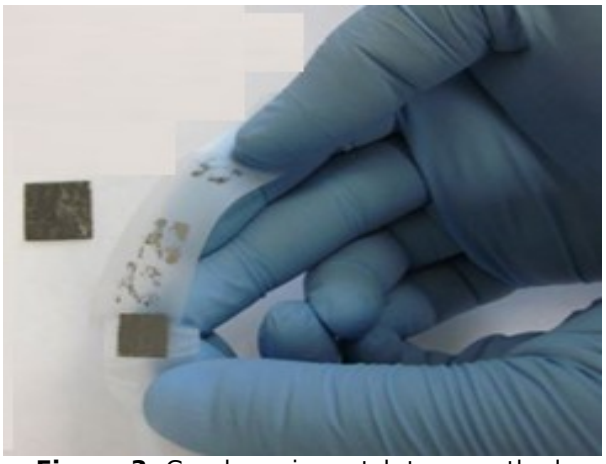

Figure 3: Graphene in scotch tape method.

2.1.4. Synthesis of graphene nanoribbons and nanographene flakes

The substrate used for on-surface synthesis normally involved a clean single-crystalometalic surface of Au, Ag, Cu, Ni, Pt etc. Metal surface act as both catalytic support and template to facilitates the absorption, chemical transformation and re-organization of molecular precursors into the required product. Various chemical reactions including aryl-aryl coupling, glaser coupling, radial polymerization, and oxidative cyclo-dehydrogenation, are used in the strategies to prepare the surface assisted transformation. Such an approach is frequently used for the synthesis of graphene nanoribbons (GNRs) and nanographene flakes (49).

2.2. Synthesis Process of Graphene Oxide

2.2.1. Improved Hummer's method

There are two main problems arose in Hummer's method (51-53). First one is intercalating agents and high consumption of oxidants was inevitable. Secondly it is a time-consuming process. Both these problems result in poor scalability and high cost in practical applications. Hence an economical and efficient method was demanded, which is popularly known as improved Hummer's method. In 2016, Huitao Yu et al. (52) had used improved Hummer's method for the synthesis of GO where they took boric acid (H_3BO_3) in place of $NaNO_3$, partly replaced $KMnO_4$ with K_2FeO_4 and reduced the amount of sulphuric acid. They first took 10 g of graphite flake, 6 g of $KMnO_4$, 4g of Potassium Ferrate (K_2FeO_4), 0.01 g of boric acid (H_3BO_3) and then dispersed the mixture in 100 mL of conc. H_2SO_4 in a vessel and stirred for 1.5 hours at less than 5 °C. Further they added $KMnO_4$ and put the vessel into a water bath at about 35°C and stirred for 3 hours more to complete the oxidation process. Then they added 250 mL of deionized water slowly adjusting the temperature to about 95°C and kept for 15 minutes, when the brownish suspension was yielded indicating the hydrolysis and absolute exfoliation of intercalated graphite oxide. This brown suspension was then treated with 12 mL of H_2O_2 (30%) to reduce the residual oxidants and intermediates to soluble sulphate. After it was centrifuged at 10,000 rpm for 20 minutes to remove the residual graphite and then washed with 1 mL/L HCl and deionized water repeatedly, and finally GO was obtained. It is the improved Hummer's method where sodium nitrate is replaced by H_3PO_4 (phosphoric acid) with an extra amount of $KMnO_4$. There is no evolution of toxic gases in this method and provides easy temperature control and GO powders with a high degree of oxidation are then resulted (53–61).

2.2.2. Modified Hummer's method

This method is the modified synthesis route proposed by Hummer. This was employed by Jianguo Song et al. (51) to synthesize GO. They combined 108 mL of H_2SO_4 and 12 mL of H_3PO_4 with 5 g of graphite and 2.5 g of $NaNO_3$ and then swirled the mixture for 10 min in an ice bath. The liquid was then progressively heated to below 5°C while 15 g of $KMnO_4$ was added. The suspension was then chilled for 2 hours, swirled for 60 minutes, and then stirred once more for 60 minutes in a water bath of 40°C. They continued adding water with a temperature of about 98 °C for 60 minutes. To make the suspensions volume 400 mL, more deionized water was added with it. An amount 15

mL of H_2O_2 was then added after 5 minutes. The final product was centrifuged and repeatedly rinsed with deionized water and a 5 % HCl solution. The product was then dried at 60 °C to synthesize GO (58-63).

2.2.3. Electrochemical method

Being ecofriendly, highly efficient, and low cost, electrochemical (EC) methods have been widely used now for the purpose of GO synthesis. Songfeng Pei *et al*. (57) were used electrochemical method in which they used flexible graphite paper (FGP) as a raw material. The FGP has similar structure as graphite, high tensile strength, and electrical conductivity. They dipped FGP slice having dimension 10 x 4 cm^2 into 200 mL concentration H_2SO_4 for EC intercalation. During EC intercalation FGP slice and Pt wire were used as anode and cathode respectively with a DC power supply of 1.6 V and found graphite intercalation compound paper (GICP). Then the GICP was subjected EC oxidation in diluted H_2SO_4 (50wt.%) where GICP and Pt wire were used as anode and cathode, respectively, with a DC power supply of 5 V. Then the blue-coloured GICP was turned to yellow coloured graphite oxide within a few seconds along with exfoliation indicating a quick oxidation and exfoliation. The exfoliated graphite oxide was collected by vacuum filtration. Then they washed the obtained filter cake with distilled water several times to clean the absorbed acid and finally GO was obtained.

2.2.4. Modified Marcano's method

The presence of Mn residues, emission of toxic gases (such as NO_2 and N_2O_4) and the explosive nature of reactions was prevailing while synthesizing GO. Keeping this in mind, Marcano et al. (37) modified Hummer's method, i.e., Marcano's method, where they claimed total elimination of Mn residues as well as toxic gas generation. Ranjan et al. (56) also used Marcano's methods with some modifications to prepare GO.

3. RESULTS AND DISCUSSION

The real image of graphene is displayed in Fig. 4. For the structure analysis of the grapheme-based materials, X-Ray Diffraction & Raman Spectroscopy were taken.

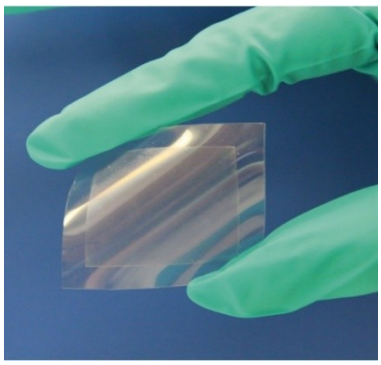

Figure 4: Real image of graphene.

3.1. Characterization Using XRD

3.1.1. Graphene Nano sheets (62-65)

Materials used - Spectral graphite (50 µm), distilled water, aqueous solution of resistivity 18.2 MΩ, ammonia, hydrazine hydrate, K_2HPO_4/KH_2PO_4. Synthesis method: Graphene was synthesized using Modified Hummers' method. Instrument model: XRD patterns were taken using SRD-6000 X-Ray diffractometer (Shimadzu, Japan) by Cu – Kα radiation. Results: XRD pattern of graphene was observed having a high peak at Bragg angle of 2Θ=26.6° having inter planner spacing value (*d*)= 0.335 nm of plane (002).

3.1.2. Reduced GO (rGO) using different treatments of GO (63-66)

Materials used- Graphite (purity of 99%), H_2SO_4 (98% purity) and H_2O_2 (30% purity), $KMnO_4$, L-ascorbic acid (purity 99%) and ethylene glycol. Synthesis method: Graphene oxide (GO) was prepared in sonication method and rGO was formed then. Instruments used: XRD (D/Max 2200V/PC, Rigaku, Japan) where Cu – Kα has the wavelength (λ= 0.15 nm) using 2Θ ranging (5°-80°) at a scanning rate of 2°/ min where voltage and current values were 40 kV and 40 mA, respectively. Results: XRD was done to find if any changes occur to the structure crystal after the conversion of graphene-to-graphene oxide and after the reduction of GO to rGO. It can be seen that the graphene shows a high intensity and sharp peak at 2Θ value 24° to 28° which shows large crystallite size and crystallinity morphology of graphite.

3.1.3. GO Nanosheets via modified Hummers' method (62, 67)

Materials used- purified graphite powder, 35% hydrogen peroxide (H_2O_2), sodium nitrate ($NaNO_3$), 37% HCl, $KMnO_4$, and 95%–97% concentrated H_2SO_4. Each chemical was at analytical quality. Synthesis method: The GO was synthesized by oxidation via modified Hummer's method. Instruments used: High Resolution XRD (Bruker D8 Advance) where Cu-Kα (λ= 0.154 nm) radiation in 2Θ ranging between 10° to 40°. Structural analysis: The interlayer changes and crystalline properties of GO were observed by XRD. Here a high diffraction peak was observed near 12° which has base plane (002) and appx. 0.737 nm d-spacing. The presence of oxygenated functional group on GO during oxidation of graphite powder made large interlayer spacing of GO. This result was proved the formation of GO.

3.1.4. Thermal reduction of GO: Chemicals used (68)

Powdered graphite (98%), H_2SO_4 (98%), fuming nitric acid (68%), pure $KMnO_4$, hydrogen peroxide (30%), ortho phosphoric acid (88%), HCl (35%) and ethanol. All materials were analytical grade. Synthesis method: GO was synthesized in Tour's method and exfoliation of GO produces rGO. Analysis: XRD pattern was observed from GO and rGO by using powder XRD under Cu-Kα (λ = 0.154 nm) of radiation in 2Θ in range 10° to 90° where the step size is 0.05° and a time per step of 0.4 sec. Structural analysis: Here also in the conversion from GO to rGO, the first peak was observed in between 20° to 30° (in 2Θ). With the change in d-spacing, a shift in first major peak was observed. The second major peak gets flattened with increase of reduction temperature. In all rGO specimens, the presence of (002) and (100) planes were found.

3.1.5. Thermal and morphological study of graphene based polyurethane composites (68-70)
Materials used- graphene, Pearl bond DIPP 119 Polyurethane, and n-Dimethyl formamide (DMF). Preparation method: with varying weight percentages of graphene of 2.5, 5 and 10 wt percent, polyurethane nanocomposites (PU025, PU050, and PU100) were created by melt mixing in the presence of a solvent, and films were created using the solvent casting method. Instrument model: XRD - D8 advance, Bruker, Germany. The analysis was conducted in the range of 2Θ = 10° to 60° at 0.03 s per step in one scan. Results: the presence of graphene in the nanocomposite was studied using XRD patterns where the highest peak was found at around 20° value of 2Θ of (110) crystalline plane. For pure graphene, the highest peak was observed at 2Θ ~27°.

3.1.6. Graphene films by modified hummer's method (71-76)
Materials used- graphene flakes (99.8% pure), $KMnO_4$ (98.5% pure), H_2SO_4 (98% pure), hydrofluoric acid (40% pure), hydrogen peroxide (30% pure), hydrochloric acid (35-37% pure), $NaNO_3$ (98% purity), acetone, distilled water and deionized water. Synthesis method: Graphite flakes were purified and then synthesized to GO by modified hummer's method. Results: at 2Θ ~ 10°, a diffraction peak of GO was observed with interlayer spacing, d = 0.8 nm with miller indices (001). But with interlayer spacing, d = 0.34 nm of indices (002), the diffraction peak was observed at 2Θ ~ 26°. In case of dried GO, the main peak of graphite vanishes totally and this peak was broader and lower in intensity than the natural graphite.

3.1.7. Reduced graphene oxide by modified Hoffman method (71-74)
Materials used- graphite powder, $KClO_3$, $NaBN_4$, H_2SO_4, H_2O_2, HCl, diethyl ether, distilled water, HNO_3. Synthesis method: Modified Hoffman method was used for the preparation of rGO and was compared with conventional Hoffman method. XRD model: the diffraction pattern of the powder rGO was observed by using Philips X'pert pro PMD (operated at 40 kV and 30 mA) with Cu-Kα radiation at 2Θ range from 20° to 80° in continuous mode. Results: when GO and rGO were processed through modified Hoffman method and conventional Hoffman method then the XRD pattern showed its peak at Bragg's angle 2Θ value of 26° with inter planner spacing, d at 0.33 nm and the miller indices (002). After chemical oxidation an additional peak was formed having Bragg's angle value 2Θ = 12.30° (approx.) and d = 0.73 nm.

3.1.8. Comparative study of different scalable routes to synthesize graphene oxide and reduced graphene oxide (71-73)
Materials used-graphite powder (<20μm), HCl (37%), $KMnO_4$ (99%), H_2SO_4 (96%), H_2O_2(33%), ethanol (99.5%), K_2FeO_4 (92%). Preparation method: Graphite Oxide was first synthesized using improved Hummer's method and also using ferrate method XRD model: The X-Ray diffraction pattern was observed using a PHILLIPS, PW-1171 with Cu-Kα radiation λ = 1.5404 Å. Results; the XRD pattern observed for the GO synthesized using Modified Hummer's method has a sharp peak at Bragg's angle value 2Θ = 26.5° where the plane has indices (002) and the inter planner spacing d = 0.34 nm. Whereas for the GO synthesized using ferrate method, the graph observed using XRD pattern has a high peak at Bragg's angle value at 2Θ = 26.6°.

3.1.9. Graphene nanostructures via arc discharge method (74, 75)
Materials used- composition of graphite electrodes (99.99% purity), buffer gasses (He and N_2). Preparation: Arc discharge method was used to synthesize pure carbon nanostructures in a stainless-steel reactor. There was a stainless-steel reactor connected to a DC power supply and buffer of mixture of gases of nitrogen and helium. On managing the distance between anode and cathode, a constant discharge current of 150 A was set. By continuing the process for 10-12 minutes, the anode graphite rod was consumed completely. After each stage of complete discharge pulse, the black carbon shoot was collected from the anode. Instruments used: The X-Ray diffraction was conducted using a Bruker™ D8 Advance series diffractometer with Cu-Kα radiation at a range of 2Θ value from 10° to 90° (λ = 1.5406 Å) at 35 kV, 40 mA operating at a speed of 2° per minute. Results: The X-Ray diffraction showed a highest peak of Braggs angle value 2Θ= 12.85° for inter planner spacing value 9.141 nm with indices of the plane (002).

3.1.10. Synthesis and characterization of graphene oxide nanosheets (76, 77)
Materials used- H_2SO_4, $KMnO_4$, deionized water. Synthesis method: GO was synthesized using Modified Hummer's Method. XRD model: XPERT-PRO diffractometer was used, operating at 40 kV and 30 mA, the XRD pattern was observed in the Bragg's angle 2Θ at range of 5°-50°. Result: after the chemical oxidation of GO the XRD pattern showed the highest peak at Bragg's angle value 2Θ =10.40° and d = 0.846 nm for (001).

3.1.11. Highly controllable and green reduction of graphene oxide to flexible graphene film with high strength (77-79)
Materials used- sodium citrate, carboxyl group, sodium borohydride. Synthesis method: Modified Hummer's method was used to synthesize the graphite oxide and its exfoliation was done by ultra-sonication method for 30 minutes and GO was formed. XRD model; the morphology of the powder was formed by Rigaku D/Max-2400X where Cu-Kα radiation was at 40 kV and 100 mA. Results: in the reduction of GO to CCG a continuous reaction occurred and at first when GO was examined by XRD analysis and patterns were observed, it showed a high sharp at Bragg's angle value of 2Θ = 11° where the inter planner spacing (d) was 0.758 nm and the indices of the plane was (001). After 1 h, a broad peak appeared at 2Θ = 24° with (002).

Table 1: Variation in Bragg's angle (2Θ) and inter planner spacing (d) in different synthesis methods observed through XRD.

Sl. No	Materials used	Instruments	Synthesis Method	Results	Reference
01	Spectral graphite, distilled water, aq. Solution (18.2 MΩ), NH_3, K_2HPO_4 / KH_2PO_4	SRD-6000 X-RAY Diffractometer	MHM	2Θ = 26.6° d=0.335 nm (002)	(62)
02	Graphite, H_2SO_4, H_2O_2, $KMnO_4$ Ascorbic acid, ethylene glycol	D-MAX 2200 V/PC 40 kV-30 mA	Sonication Method	2Θ = 9° d=7.37 nm (002) 2Θ = 26.7° d=3.35 nm	(63)
03	Graphite powder, H_2O_2, $NaNO_3$, HCl, $KMnO_4$, H_2SO_4	Bruker D8 Advance	MHM	2Θ =12° d =7.37 nm (002)	(55)
04	Graphite, H_2SO_4, HNO_3, $NaNO_3$, $KMnO_4$, H_2O_2 Orthophospheric acid, HCl	PANALYTICAL XPERT^3 Powder diffractometer	Tour's Method	2Θ = 25° (002)	(64)
05	Pearl bond DIPP 199, polyurithene, n-Dimethyl formide	D8 advance Bruker, Germany	Polyurithene nanocomposites fabricated using melt mixing & flims were fabricated in solvent casting method	2Θ = 20° (110) 2Θ = 27° (001)	(68)
06	Graphite powder, $KClO_3$, $NaBN_4$, H_2SO_4, H_2O_2, HCl, HNO_3	PHILLIPS XPERT PRO PMD 40 kV-30 mA	MHM Conventional HOFFMANN Method	2Θ = 26° d = 0.33 nm (002)	(73)
07	Graphite powder, HCl, $KMnO_4$, H_2SO_4, H_2O_2, ethanol, K_2FO_4	PHILLIPS PW-1171	Improved HM Ferrate Method	2Θ =26.5° d = 0.34 nm (002)	(74)
08	Graphite, Nitrogen (N_2) Helium (He)	Bruker™D8 Advance series 35 kV – 40 mA	Arc discharge Method	2Θ = 12.85° d = 0.914 nm (002)	(75)
09	H_2SO_4, $KMnO_4$, Deionised water	GO XPERT-PRO 40 kV-30 mA	MHM	2Θ =10.40° d = 0.846 nm (001)	(76)
10	Sodium nitrate, carbonyl group, Sodium Borohydrate	D/MAX-2400X 40 kV – 100 mA	MHM	2Θ = 24° (002) 2Θ =11° (001)	(77)
11	$Ni(NO_3)_2.6H_2O$, $Co(NO_3)_2.6H_2O$, $C_2H_6O_7$, $LiNO_3$	XRD-600, 40 kV – 30 mA	CVD	2Θ = 26.6° d = 0.335 nm (001)	(78)

3.1.12. Improvement of Li-ion batteries energy storage by graphene additive (78, 79)
Materials used- $Ni(NO_3)_2 \cdot 6H_2O$, $Co(NO_3)_2 \cdot 6H_2O$, $C_6H_6O_7$and $LiNO_3$ (everything were of 99.99% purity) and were received from m Harris Chemicals Corporation in England, deionized water. XRD model: The X-Ray diffraction was performed by XRD-6000 of 2Θ operating at 40 kV and 30 mA were using Cu-Kα (λ = 0.154 nm). Results: the XRD pattern of pure graphene doped with LCNOG at 850°C has a high peak at 2Θ = 26.6° with d = 0.335 nm for (003).

The above said results of interplanar spacings (d) and their corresponding Bragg's angles (2Θ) are displayed in Figure 5, and the summary of XRD characterization results were presented in Table 1.

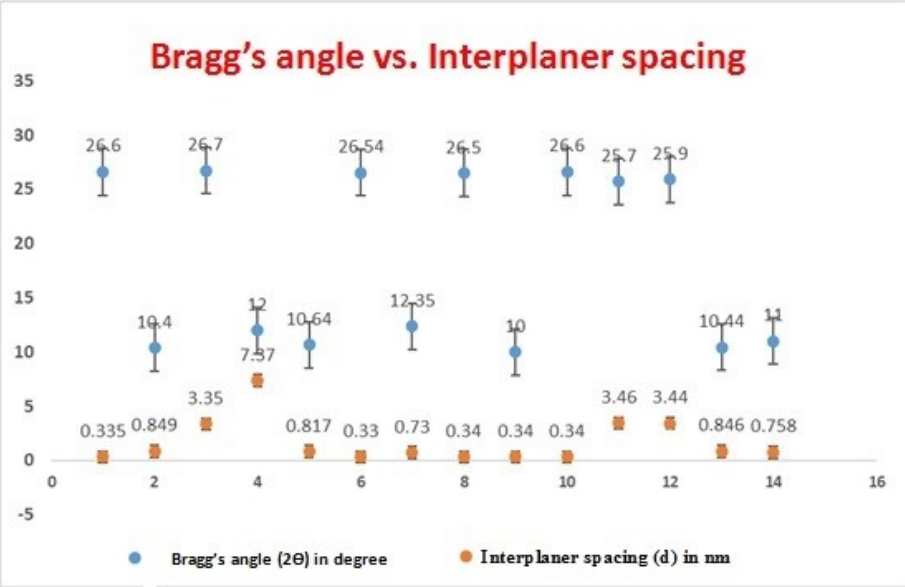

Figure 5: Variation of interplanar spacing with respect to Bragg's angle.

3.2. Characterization Using Raman Spectroscopy

Raman spectroscopy is typically preferred to evaluate the changes that take place during oxidation and exfoliation. Graphene was produced from GO using the modified Hummers method by Fatima Tuz Johra et al. (79). One D band was found at 1353 cm^{-1}, whereas the G band found at 1605 cm^{-1} of GO, which corresponds to the E_{2g} phonon of the sp^2 C atoms. However, the G band in the instance of graphene was around 1600 cm^{-1}, indicating a minor displacement from the GO's position. The D band is a sign of disorder and can be caused by a number of flaws, including vacancies, grain boundaries (79-82) and amorphous carbon species (83, 84). The product's quality is indicated by the intensity ratio of these two bands. Relative intensity (I_D / I_G) dropped from 1.00 to 0.96. The I_D / I_G ratio of reduced graphene oxide treated with hydroiodic acid and acetic acid was increased (85, 86), showing that the reduction process changed the structure of GO and caused a significant number of structural flaws (86- 88)

GO was obtained from Graphene as a 0.4 weight percent water solution with a reported monolayer content > 95 percent by V. Scardaci and G. Compagnini (84, 85). After a 30-minute ultrasonic bath, the solution was applied. Raman spectroscopy was used to assess the acquired rGO's quality by contrasting it with GO and various scanning speeds. The G and D bands visible in these spectra are typical carbon nanostructures. The degree of disorder has been calculated inside the material using relative intensity (I_D / I_G) (85-88). Raman spectroscopy was used to assess the quality of the obtained material after a thorough investigation of the laser reduction of GO under a variety of experimental conditions. The scan speed is an important parameter because a slow speed would have a negative impact on the material's quality, while material density was found to have less of an impact. For greater density samples, a second laser pass over a surface that has already received treatment improves the final rGO quality. Modified Tour's method for the synthesis of GO was used by Iman Sengupta et al. (64) and then followed thermal reduction method to form graphene from GO. They captured these peaks for three samples since the D and G peaks are the specific characteristics of carbon compounds, presented in Table 2.

Table 2: Raman spectroscopy data for different samples (64).

Sample Name	D-peak (in cm^{-1})	G-peak (in cm^{-1})
Graphite	1352	1580
GO	1370	1608
Laser modified GO	1370	1608

The above table makes it clear that due to graphite oxidation and exfoliation, there is a notable reduction in the size of sp^2 planes. After the lowering of GO, the intensities of the D and G peaks both raised, and the peaks are sharpened, indicating a structural shift.

Modified Hummer's approach for the synthesis of GO was used by MF Hanihah et al. (87). Raman analysis of GO was performed in order to evaluate its structural and electronic properties because it is a non-destructive method, and the results are shown in the Table 3.

Table 3: Raman spectroscopy data for GO (87)

Sample Name	D-peak in cm^{-1}	G-peak in cm^{-1}	I_D / I_G
GO	1353	1600	0.90

Elvin Aliyev et al (88) produced base washed GO using Hummer's method for its synthesis by dispersing GO in 1.0 M sodium hydroxide, shaking for 3 hours, refluxing for an hour at 80 °C, and vacuum-filtering to remove 30 weight percent of oxidative debris from the CGO dispersion. Following the creation of reduced GO and reduced base washed GO separately, they dispersed 2.0 g of each in 1.0 L of ultrapure water in two separate flasks, sonicated the mixture, and then reacted with 10 mL of hydrazine monohydrate at 100°C for an entire day. They had produced base washed GO by dispersing GO in 1.0 M sodium hydroxide and shaking for 3 hours. They followed Hummer's method for the synthesis of GO (87, 89).

For the pure graphite, they discovered D-peak and G-peak at 1360 and 1580 cm^{-1}, respectively. When graphite is converted to GO, it is found that the degree of order in the structure has changed; the intensity of the D-band is higher than it is for graphite, and the intensity of the G-band is lower for reduced forms. Between 1342 cm^{-1} and 1356 cm^{-1}, D peak appears in oxidized forms. Thus, they demonstrated that GO samples have a massive number of flaws and are in a distorted version of the sp^2 crystal structure. The activation of the D peak typically takes place in crystal areas of 3–4 nm size that are near flaws or an edge (90-92). The activation of 2D and 2D' bands doesn't require any faults (93). As a result, figuring out the number and orientation of graphene layers can be helped by the 2D peak's (2700 cm^{-1}) structure. Single-layer graphene is thought to exist if there is a single sharp peak at the 2D-band peak. Graphene oxide samples in bulk form were employed in the studies, and the findings indicate that there are numerous single layers in the GO samples. This result indicated that exfoliation was necessary in order to obtain single-layer GO layers from the graphene oxide samples which they had synthesized.

Bilayer graphene film was made on commercial Cu (0.5% Ni) foil (92, 93). Cu (0.5% Ni) foils were put into an AP-CVD quartz tube set up for monolayer and bilayer graphene synthesis before cleaning and removing any residue with the electro polishing procedure. The graphene films were subsequently applied to SiO_2/Si substrates that were 300 nm thick. Raman spectroscopy was used to analyse graphene / SiO_2 /Si samples (graphene films). The result of Raman spectra is summarized in Table 4.

Table 4: Raman spectroscopy data for graphene.

Sample Name	D-peak in cm^{-1}	G-peak in cm^{-1}	2D-peak in cm^{-1}
Graphene	1350	1590	2690

For the creation of graphene on 4H-SiC (001) semi-insulating on-axis, K. Grodecki et al. (94) utilized a commercial horizontal CVD hot-wall reactor (Aixtron VP508). Lorentz fitting had employed for the area and FWHM of the 2D band to calculate the thicknesses of graphene structures. Wire 3.4 software was used to measure both metrics. The values of FWHM for 2D bands different layers of graphene structures are presented in Table 5.

Table 5: Raman spectroscopy data for different samples.

Number of layers in Graphene	Range of FWHM in cm^{-1}	Number of Lorentzian peaks fitted
Monolayer (ML)	30-45	1
Bilayer (BL)	45-60	4
Trilayer (TL)	60-75	3

The regions marked as ML have a smaller 2D area than regions marked as bilayered, trilayered, and tetralayered graphene.

By following the improved Hummers method for the synthesis of GO, B. Dehghanzada et al. (95) employed hydrazine hydrate to reduce GO. They dispersed GO and dodecyl amine in 200 mL of DMF for the Synthesis of functionalized GO (FGO).

To create reduced functionalized graphene oxide (rFGO), they used hydrazine hydrate as a reducing agent. Rapid thermal processing of GO produced exfoliated graphene sheets, which were then used to create thermally reduced GO (TRG). The corresponding data of Raman spectra of pure graphite, GO, FGO, rFGO and TRG samples are presented in the Table 6.

Table 6: Raman spectroscopy data for different samples.

Sample	D-peak in cm^{-1}	G-peak in cm^{-1}	I_D/I_G	L(Å) $=44/(I_D/I_G)$
Graphite	1360	1580	0	--
GO	1284	1597	1.54	28.57
FGO	1289	1586	1.57	28.02
RFGO	1330	1582	1.6	27.5
TRG	1290	1580	1.75	25.14

The important parameter in Raman spectroscopy is the determination of the intensities of D-peak to that of G-peak (I_D/I_G) in order to examine the level of modification of pure graphite following oxidation as

well as reduction. I_D/I_G is zero for pure graphite, indicating that there are no flaws in the material.

The following equation, provided by Tuinstra et al. (80) was used to calculate the average distance (L) between two neighbour defects, L (Å) = 44/ (I_D/I_G). An increase in the I_D/I_G ratio indicates that there are more faults and that the distance between each defect is getting closer.

For the synthesis of GO, A. Malas et al. (53) used a modified version of the Hummers method and used a variety of techniques for reduced GO. First approach: It involved the reduction by sodium borohydride ($NaBH_4$) to obtain the end product i.e., $NaBH_4$reduced GO (NarGO). Second approach: The reducing agent in the second process was hydrazine monohydrate ($N_2H_4.H_2O$) to obtain $N_2H_4.H_2O$ reduced GO (HyrGO). Third approach: NarGO was transferred into a new round-bottom flask containing 300 mL of water, and the second reduction method's steps were then carried out with the aid of 3 mL of $N_2H_4.H_2O$. NaHyrGO is the abbreviation for the final product following two treatments with two reducing agents. Fourth approach: They performed thermal treatment to generate thermally reduced graphene oxide (TrGO).

In order to study the relative contributions of ordered and disordered regions in carbonaceous structures, Raman spectroscopy is frequently regarded as a significant instrument. Summarizing the results of Raman spectra of graphite, GO and the reduced GO generated by different ways (63, 71, 96), presented in Table 7.

Table 7: Raman spectroscopy data for different samples.

Sample	D-peak in cm^{-1}	G-peak in cm^{-1}	I_D/I_G
Graphite	1328	1573	0.19
GO	1335	1602	1.10
NarGO	1327	1598	1.24
HyrGO	1327	1596	1.27
NaHyrGO	1328	1586	1.35
TrGO	1344	1597	1.02

The size of the sp^2 hybridized carbon atoms is inversely proportional to the ratio of the intensities of the D-peak and G-peak, or relative intensity (I_D/I_G). Since it is clear from the above table that all chemically reduced GO have relative intensities that are higher than GO. It is important to note that, with the exception of thermally reduced GO, the size of sp^2 hybridized carbon atoms decreases throughout reduction. The authors speculate that the relative intensity of thermally reduced GO is lower than that of GO. The removal of oxygen groups may result in dangling bonds that introduce sp^3carbons. It has been established that a reduced GO Raman spectra with a lower relative intensity compared to GO denotes defect correction and a greater distance between them (87, 95).

In order to manufacture the three different forms of graphene oxides—GO1, GO2, and GO3, M. Wojtoniszakand and E. Mijowska (96) had employed three distinct techniques. The following steps were used to prepare GO1: 1 g of graphite was dissolved in 350 mL of a 4:3 volume ratio mixture of perchloric and nitric acids, and then 6 g of K_2CrO_4 was added. After that, the mixture was heated to 50°C, and the reaction was run for 24 hours. The resulting mixture was then passed through a polycarbonate (PC) membrane and washed three times with ethanol and 10 percent hydrochloric acid to remove any remaining metal ions. Finally, distilled water was added to the mixture until the pH level reached 7. The material was then dried in the air for 24 hours at 100°C. rGO1, rGO2, and rGO3 are the equivalent reduced graphene oxides.

To prepare GO2, graphite, perchloric acid, nitric acid, and K_2CrO_4 were mixed and then heated. This procedure took place at room temperature for 6 hours. Following the oxidation process, the same methods of purification, filtration, and drying as in the previous procedure were used to produce GO2.

To prepare GO3, the same steps as for second type synthesis were used, with the exception that the oxidation process' time and temperature were increased to 48 hours and 100°C. Here, glucose was employed as a reducing agent in the preparation of rGO1, rGO2 and rGO3.

Characterization of Raman: One 2D band of two and more layered graphene is composed of two halves, 2D1 and 2D2. As the number of layers rises, both the blue shift of the 2D peak and the relative power of the 2D2 peak both noticeably increase. However, graphene with a single sheet only shows a single 2D peak. Graphite has a single 2D peak. Additionally, rGO3 only has one 2D peak, and their individual values. rGO3 is single layered whereas other two types reduced graphene oxides (rGO1 and rGO2) are composed of multi-layers.

4. APPLICATIONS

Graphene is flexible and transparent (Fig. 6) and has various applications due to its unique structures and properties.

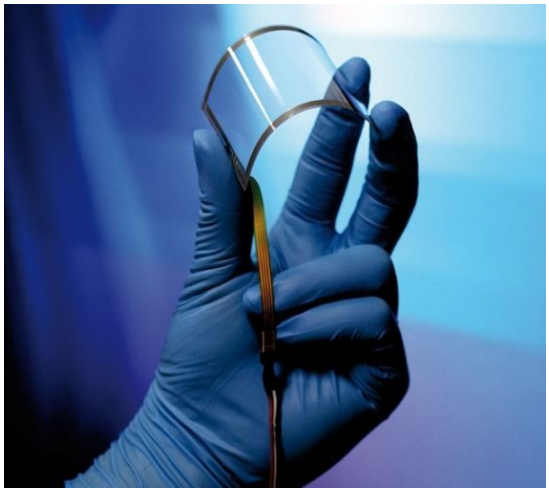

Figure 6: Graphene used as smartphone screen.

4.1. Graphene Transistors: Development of GFETs (graphene field effect transistors)

There are two familiar transistors, i.e., analog transistors and logic transistors. In order to get low energy consumption and to maintain a high interpretation, earlier it is characterized by a high I_{on}/I_{off} ratio and later it is used as an amplifier in high frequency application. Electrical property of graphene is used in both logic and analog transistor (49-54, 59).

4.1.1. Logic transistor

With the fabrication of MOSFET, CMROs technology has dominated the logic industry for around 40 years. By reducing the length of transistors gate we can get higher transistor density and high electrical fields in channel region but when the size is reduced, problems arise like hot electron effect, velocity saturation effect and punch through effect. Due to its monoatomic thickness, graphene reduces all these effects providing a high mobility channel. For modifying a graphene bandgap several techniques are used.

4.1.1.1. Bilayer graphene

By using the application of transverse electric field these structures allow opening of band gap as the symmetry of bilayer stack breaks. SiC is the substrate used by bilayer graphene where light doping is provided to the bottom graphene layer by the substrate and by the adsorption of potassium atoms upper graphene layer is doped. This material is used by several groups for the design of FET devices.

4.1.1.2. Graphene nanoribbons

Graphene nanoribbons are also used to modify graphene. Here the graphene plane is engineered and an extra charge carrier sheet is added. It remains one dimensional and the confinement opens a transport gap.

4.1.1.3. Nano-mesh graphene

Pattern hole in a graphene sheet is another way of including a bandgap in graphene. The required I_{on}/I_{off} ratio for this technique is of the order of 100 at room temperature for size of patterned holes approximate 7 nm. When the on-off ratio increases, at the same time neck width of the hole decreases. Scalability is the main advantage of this technique.

4.1.1.4. Graphene nano bubbles

Several studies show engineering from graphene nano bubbles introduces bandgap by taking psudo magnetic fields which results Landau quantization. By patterning a substrate of holes or steps, nanobubbles can be formed, with substantial energy gaps exceeding 0.1 eV margin.

4.1.2. Analog transistor

Other type of transistor is the analog transistor. The logic transistor is not used in this device and bandgap also not required. They are used in radio frequency applications. Graphene is the most important material for making analog transistor due to its high cutoff frequency.

4.2. Optoelectronics

Optical properties; Graphene used in optoelectronic devices. Graphene has high transparency low reflection, high carrier mobility and near ballistic transparent at room temperature. Due to these properties, graphene used as transparent electrodes. High absorption is another property of graphene which can be described by its structure constant α (constant, shows interaction of matter and electromagnetic field). Absorption of FLG is proportional to number of layers of graphene used in many optoelectronic and photonic devices, also used in photodetectors, structurable absorbers and optical limiters.

Transparent conducting electrodes; These are mostly used in academic and industrial settings to commercial devices. Initially they worked by inserting charge according to the device. In some part of electromagnetic spectrum, they are highly translucent. ITO (Indium Tin Oxide) is the mostly used material for TCEs. It is very costly because of the low supply of Indium. Benefits of organic TCEs are low cost, flexibility and stability but they are unable to acquire the amount of charge mobility as inorganic material. Graphene as TCE; high optical transmittance and low sheet resistance are most essential parameters of TCE materials. By using a four-terminal sensing measurement technique, the sheet resistance can be obtained. In most cases graphene either matches or exceeds the transmittance of other materials.

4.3. Graphene Sensor

Graphene used in sensor application because of its highly reactivity to adsorbed materials.

Electrochemical sensor; As compared to Graphite, glassy carbon electrodes and CNTs, graphene shows better electrochemical response. Researchers proved that at 7.0 pH value of phosphate buffered saline solution graphene showed electrochemical potential window of ca. 2.5 V in 0.2 m. When CNTs decorated with nanoparticles it can detect gasses. Researcher demonstrates that rGO can detect poisonous gas with ppb sensitivity. rGO based sensor and CNT based sensor have same performance. The only difference is rGO based sensor release very less noise.

4.3.1. Graphite as a biosensor

The electrode reaction of hydrogen peroxide on rGO is highly efficient as compared to glassy carbon,

graphite and CNTs. It is same as the reaction of NADH on graphene-based electrodes. As compared to the bare edge plane pyrolytic graphite electrode (EPPGE), oxidation of NADH on graphene is strongly observed. As compared with ascorbic acid, dopamine and serotonin, graphene shows superior sensing ability.

5. CONCLUSIONS

Graphene is being exhibited a huge number of amazing electrical and physical properties. Graphene and graphene oxide (GO) shows less similarly with most number of the artificial compound. A variety of synthesis methods for graphene and graphene oxide were discussed, i.e. top-down synthesis, bottom-up, mechanical delamination, π magnetism, exfoliation and cleavage method. It is found that CVD technique is the most suitable for the synthesis of high quality graphene. CVD method is commercially usable and trustable for the application of GNRs. Researchers developed different methods of production which was suitable for cost, scalability and environment friendly. GO based graphene synthesis method produced low quality graphene leading to low conductivity. Good quality graphene can be obtained from electrochemical exfoliation process, which also mostly used in industrialization. In this review we have discussed the importance of graphene in different fields due to its application in biomedical science, weather proofing and packaging, transistor, semiconductor, super capacitor, rust free future, sensor and optoelectronics. The results of different samples, characterized by XRD and Raman Spectroscopy were discussed in this review article.

6. CONFLICT OF INTEREST

No conflict of interest.

7. ACKNOWLEDGEMENTS

The authors are grateful to the President, Vice President and Registrar of GIET University, Gunupur for motivation. The authors are thankful to Prof. B. B. Swain for his useful input in preparing the review article.

8. REFERENCES

1. Kuanar B, Mohanty HS, Behera D, Nayak P, Dalai B. An elementary survey on structural, electrical, and optical properties of perovskite materials. Eng Appl Sci Res [Internet]. 2022;49(2):288–99. Available from: <URL>.

2. Dash S, Hial PK, Senapati S, Dalai B. A Survey on Various Methods of Extraction and Recovery of Thorium. J Turkish Chem Soc Sect A Chem [Internet]. 2021 Nov 30;8(4):1197–210. Available from: <URL>.

3. Novoselov KS, Geim AK, Morozov S V., Jiang D, Zhang Y, Dubonos S V., et al. Electric Field Effect in Atomically Thin Carbon Films. Science [Internet]. 2004 Oct 22;306(5696):666–9. Available from: <URL>.

4. Novoselov KS, Fal'ko VI, Colombo L, Gellert PR, Schwab MG, Kim K. A roadmap for graphene. Nature [Internet]. 2012 Oct 10;490(7419):192–200. Available from: <URL>.

5. Peigney A, Laurent C, Flahaut E, Bacsa RR, Rousset A. Specific surface area of carbon nanotubes and bundles of carbon nanotubes. Carbon [Internet]. 2001 Apr 1;39(4):507–14. Available from: <URL>.

6. Gadipelli S, Guo ZX. Graphene-based materials: Synthesis and gas sorption, storage and separation. Prog Mater Sci [Internet]. 2015 Apr 1;69:1–60. Available from: <URL>.

7. Bae S, Kim H, Lee Y, Xu X, Park J-S, Zheng Y, et al. Roll-to-roll production of 30-inch graphene films for transparent electrodes. Nat Nanotechnol [Internet]. 2010 Aug 20;5(8):574–8. Available from: <URL>.

8. Yang W, Ni M, Ren X, Tian Y, Li N, Su Y, et al. Graphene in Supercapacitor Applications. Curr Opin Colloid Interface Sci [Internet]. 2015 Oct;20(5–6):416–28. Available from: <URL>.

9. Tsai I-L, Cao J, Le Fevre L, Wang B, Todd R, Dryfe RAW, et al. Graphene-enhanced electrodes for scalable supercapacitors. Electrochim Acta [Internet]. 2017 Dec;257:372–9. Available from: <URL>.

10. Nag A, Mitra A, Mukhopadhyay SC. Graphene and its sensor-based applications: A review. Sensors Actuators A Phys [Internet]. 2018 Feb;270:177–94. Available from: <URL>.

11. Gusain R, Kumar N, Ray SS. Recent advances in carbon nanomaterial-based adsorbents for water purification. Coord Chem Rev [Internet]. 2020 Feb 15;405:213111. Available from: <URL>.

12. Shao C, Zhao Y, Qu L. Tunable Graphene Systems for Water Desalination. ChemNanoMat [Internet]. 2020 Jul 21;6(7):1028–48. Available from: <URL>.

13. Shen H, Zhang L, Liu M, Zhang Z. Biomedical Applications of Graphene. Theranostics [Internet]. 2012;2(3):283–94. Available from: <URL>.

14. Phiri J, Gane P, Maloney TC. General overview of graphene: Production, properties and application in polymer composites. Mater Sci Eng B [Internet]. 2017 Jan 1;215:9–28. Available from: <URL>.

15. Hu K, Kulkarni DD, Choi I, Tsukruk V V. Graphene-polymer nanocomposites for structural and functional applications. Prog Polym Sci [Internet]. 2014 Nov 1;39(11):1934–72. Available from: <URL>.

16. Geim AK. Graphene: Status and Prospects. Science [Internet]. 2009 Jun 19;324(5934):1530–4. Available from: <URL>.

17. Yu G, Hu L, Vosgueritchian M, Wang H, Xie X, McDonough JR, et al. Solution-Processed Graphene/MnO_2 Nanostructured Textiles for High-Performance Electrochemical Capacitors. Nano Lett [Internet]. 2011 Jul 13;11(7):2905–11. Available from: <URL>.

18. Liu L, Yu Y, Yan C, Li K, Zheng Z. Wearable energy-dense and power-dense supercapacitor yarns enabled by scalable graphene–metallic textile composite electrodes. Nat Commun [Internet]. 2015 Jun 11;6(1):7260. Available from: <URL>.

19. Shateri-Khalilabad M, Yazdanshenas ME. Preparation of superhydrophobic electroconductive graphene-coated cotton cellulose. Cellulose [Internet]. 2013 Apr 5;20(2):963–72. Available from: <URL>.

20. Ren J, Wang C, Zhang X, Carey T, Chen K, Yin Y, et al. Environmentally-friendly conductive cotton fabric as flexible strain sensor based on hot press reduced graphene oxide. Carbon [Internet]. 2017 Jan 1;111:622–30. Available from: <URL>.

21. Abdelkader AM, Karim N, Vallés C, Afroj S, Novoselov KS, Yeates SG. Ultraflexible and robust graphene supercapacitors printed on textiles for wearable electronics applications. 2D Mater [Internet]. 2017 Jul 24;4(3):035016. Available from: <URL>.

22. Karim N, Afroj S, Malandraki A, Butterworth S, Beach C, Rigout M, et al. All inkjet-printed graphene-based conductive patterns for wearable e-textile applications. J Mater Chem C [Internet]. 2017 Nov 16;5(44):11640–8. Available from: <URL>.

23. Lim JY, Mubarak NM, Abdullah EC, Nizamuddin S, Khalid M, Inamuddin. Recent trends in the synthesis of graphene and graphene oxide based nanomaterials for removal of heavy metals — A review. J Ind Eng Chem [Internet]. 2018 Oct 25;66:29–44. Available from: <URL>.

24. Balandin AA. Phononics of Graphene and Related Materials. ACS Nano [Internet]. 2020 May 26;14(5):5170–8. Available from: <URL>.

25. Ferrari AC, Meyer JC, Scardaci V, Casiraghi C, Lazzeri M, Mauri F, et al. Raman Spectrum of Graphene and Graphene Layers. Phys Rev Lett [Internet]. 2006 Oct 30;97(18):187401. Available from: <URL>.

26. Ferrari AC. Raman spectroscopy of graphene and graphite: Disorder, electron–phonon coupling, doping and nonadiabatic effects. Solid State Commun [Internet]. 2007 Jul 1;143(1–2):47–57. Available from: <URL>.

27. Ferrari AC, Basko DM. Raman spectroscopy as a versatile tool for studying the properties of graphene. Nat Nanotechnol [Internet]. 2013 Apr 4;8(4):235–46. Available from: <URL>.

28. He Y, Yi C, Zhang X, Zhao W, Yu D. Magnetic graphene oxide: Synthesis approaches, physicochemical characteristics, and biomedical applications. TrAC Trends Anal Chem [Internet]. 2021 Mar 1;136:116191. Available from: <URL>.

29. Chen J, Yao B, Li C, Shi G. An improved Hummers method for eco-friendly synthesis of graphene oxide. Carbon [Internet]. 2013 Nov 1;64:225–9. Available from: <URL>.

30. Brodie BC. XIII. On the atomic weight of graphite. Philos Trans R Soc London [Internet]. 1859 Dec 31;149:249–59. Available from: <URL>.

31. Singh DP, Herrera CE, Singh B, Singh S, Singh RK, Kumar R. Graphene oxide: An efficient material and recent approach for biotechnological and biomedical applications. Mater Sci Eng C [Internet]. 2018 May 1;86:173–97. Available from: <URL>.

32. Bhuyan MSA, Uddin MN, Islam MM, Bipasha FA, Hossain SS. Synthesis of graphene. Int Nano Lett [Internet]. 2016 Jun 9;6(2):65–83. Available from: <URL>.

33. Liu W-W, Chai S-P, Mohamed AR, Hashim U. Synthesis and characterization of graphene and carbon nanotubes: A review on the past and recent developments. J Ind Eng Chem [Internet]. 2014 Jul 25;20(4):1171–85. Available from: <URL>.

34. Lee HC, Liu W-W, Chai S-P, Mohamed AR, Aziz A, Khe C-S, et al. Review of the synthesis, transfer, characterization and growth mechanisms of single and multilayer graphene. RSC Adv [Internet]. 2017 Mar 9;7(26):15644–93. Available from: <URL>.

35. Shmavonyan GS, Sevoyan GG, Aroutiounian VM. Enlarging the surface area of monolayer graphene synthesized by mechanical exfoliation. Armen J Phys [Internet]. 2013;6(1):1–6. Available from: <URL>.

36. Wu YH, Yu T, Shen ZX. Two-dimensional carbon nanostructures: Fundamental properties, synthesis, characterization, and potential applications. J Appl Phys [Internet]. 2010 Oct 1;108(7):071301. Available from: <URL>.

37. Marcano DC, Kosynkin D V., Berlin JM, Sinitskii A, Sun Z, Slesarev A, et al. Improved Synthesis of Graphene Oxide. ACS Nano [Internet]. 2010 Aug 24;4(8):4806–14. Available from: <URL>.

38. Park S, An J, Jung I, Piner RD, An SJ, Li X, et al. Colloidal Suspensions of Highly Reduced Graphene Oxide in a Wide Variety of Organic Solvents. Nano Lett [Internet]. 2009 Apr 8;9(4):1593–7. Available from: <URL>.

39. Hummers WS, Offeman RE. Preparation of Graphitic Oxide. J Am Chem Soc [Internet]. 1958 Mar 1;80(6):1339. Available from: <URL>.

40. Razaq A, Bibi F, Zheng X, Papadakis R, Jafri SHM, Li H. Review on Graphene-, Graphene Oxide-, Reduced Graphene Oxide-Based Flexible Composites: From Fabrication to Applications. Materials (Basel) [Internet]. 2022 Jan 28;15(3):1012. Available from: <URL>.

41. Cockerell TDA. An Alien *Clematis* in New Mexico. Science [Internet]. 1899 Dec 15;10(259):898–9. Available from: <URL>.

42. Du W, Jiang X, Zhu L. From graphite to graphene: direct liquid-phase exfoliation of graphite to produce single- and few-layered pristine graphene. J Mater Chem A [Internet]. 2013 Aug 20;1(36):10592–606. Available from: <URL>.

43. Schniepp HC, Li J-L, McAllister MJ, Sai H, Herrera-Alonso M, Adamson DH, et al. Functionalized Single Graphene Sheets Derived from Splitting Graphite

Oxide. J Phys Chem B [Internet]. 2006 May 1;110(17):8535–9. Available from: <URL>.

44. Hlekelele L, Franklyn PJ, Tripathi PK, Durbach SH. Morphological and crystallinity differences in nitrogen-doped carbon nanotubes grown by chemical vapour deposition decomposition of melamine over coal fly ash. RSC Adv [Internet]. 2016 Aug 10;6(80):76773–9. Available from: <URL>.

45. Ye R, James DK, Tour JM. Laser-Induced Graphene. Acc Chem Res [Internet]. 2018 Jul 17;51(7):1609–20. Available from: <URL>.

46. Antonatos N, Ghodrati H, Sofer Z. Elements beyond graphene: Current state and perspectives of elemental monolayer deposition by bottom-up approach. Appl Mater Today [Internet]. 2020 Mar 1;18:100502. Available from: <URL>.

47. Hlekelele L, Franklyn PJ, Dziike F, Durbach SH. TiO_2 composited with carbon nanofibers or nitrogen-doped carbon nanotubes synthesized using coal fly ash as a catalyst: bisphenol-A photodegradation efficiency evaluation. New J Chem [Internet]. 2018 Mar 12;42(6):4531–42. Available from: <URL>.

48. Knieke C, Berger A, Voigt M, Taylor RNK, Röhrl J, Peukert W. Scalable production of graphene sheets by mechanical delamination. Carbon N Y [Internet]. 2010 Sep 1;48(11):3196–204. Available from: <URL>.

49. Song S, Su J, Telychko M, Li J, Li G, Li Y, et al. On-surface synthesis of graphene nanostructures with π-magnetism. Chem Soc Rev [Internet]. 2021 Mar 15;50(5):3238–62. Available from: <URL>.

50. Cooper DR, D'Anjou B, Ghattamaneni N, Harack B, Hilke M, Horth A, et al. Experimental Review of Graphene. Int Sch Res Not [Internet]. 2012 Apr 26;2012:501686. Available from: <URL>.

51. Song J, Wang X, Chang C-T. Preparation and Characterization of Graphene Oxide. J Nanomater [Internet]. 2014;2014:276143. Available from: <URL>.

52. Yu H, Zhang B, Bulin C, Li R, Xing R. High-efficient Synthesis of Graphene Oxide Based on Improved Hummers Method. Sci Rep [Internet]. 2016 Nov 3;6(1):36143. Available from: <URL>.

53. Malas A, Bharati A, Verkinderen O, Goderis B, Moldenaers P, Cardinaels R. Effect of the GO Reduction Method on the Dielectric Properties, Electrical Conductivity and Crystalline Behavior of PEO/rGO Nanocomposites. Polymers (Basel) [Internet]. 2017 Nov 14;9(11):613. Available from: <URL>.

54. Bhargava R, Khan S. Effect of reduced graphene oxide (rGO) on structural, optical, and dielectric properties of Mg(OH)2 /rGO nanocomposites. Adv Powder Technol [Internet]. 2017 Nov 1;28(11):2812–9. Available from: <URL>.

55. Zaaba NI, Foo KL, Hashim U, Tan SJ, Liu W-W, Voon CH. Synthesis of Graphene Oxide using Modified Hummers Method: Solvent Influence. Procedia Eng [Internet]. 2017 Jan 1;184:469–77. Available from: <URL>.

56. Ranjan P, Agrawal S, Sinha A, Rao TR, Balakrishnan J, Thakur AD. A Low-Cost Non-explosive Synthesis of Graphene Oxide for Scalable Applications. Sci Rep [Internet]. 2018 Aug 13;8(1):12007. Available from: <URL>.

57. Pei S, Wei Q, Huang K, Cheng H-M, Ren W. Green synthesis of graphene oxide by seconds timescale water electrolytic oxidation. Nat Commun [Internet]. 2018 Jan 10;9(1):145. Available from: <URL>.

58. Kavinkumar T, Manivannan S. Improved dielectric behaviour of graphene oxide-multiwalled carbon nanotube nanocomposite. Vacuum [Internet]. 2018 Feb 1;148:149–57. Available from: <URL>.

59. Jo J, Lee S, Gim J, Song J, Kim S, Mathew V, et al. Facile synthesis of reduced graphene oxide by modified Hummer's method as anode material for Li-, Na- and K-ion secondary batteries. R Soc Open Sci [Internet]. 2019 Apr 24;6(4):181978. Available from: <URL>.

60. Smith AT, LaChance AM, Zeng S, Liu B, Sun L. Synthesis, properties, and applications of graphene oxide/reduced graphene oxide and their nanocomposites. Nano Mater Sci [Internet]. 2019 Mar;1(1):31–47. Available from: <URL>.

61. Eissa S, N'diaye J, Brisebois P, Izquierdo R, Tavares AC, Siaj M. Probing the influence of graphene oxide sheets size on the performance of label-free electrochemical biosensors. Sci Rep [Internet]. 2020 Aug 12;10(1):13612. Available from: <URL>.

62. Guo H-L, Wang X-F, Qian Q-Y, Wang F-B, Xia X-H. A Green Approach to the Synthesis of Graphene Nanosheets. ACS Nano [Internet]. 2009 Sep 22;3(9):2653–9. Available from: <URL>.

63. Zainuddin MF, Nik Raikhan NH, Othman NH, Abdullah WFH. Synthesis of reduced Graphene Oxide (rGO) using different treatments of Graphene Oxide (GO). IOP Conf Ser Mater Sci Eng [Internet]. 2018 May 1;358(1):012046. Available from: <URL>.

64. Sengupta I, Chakraborty S, Talukdar M, Pal SK, Chakraborty S. Thermal reduction of graphene oxide: How temperature influences purity. J Mater Res [Internet]. 2018 Dec 14;33(23):4113–22. Available from: <URL>.

65. Dideikin AT, Vul' AY. Graphene oxide and derivatives: The place in graphene family. Front Phys. 2019 Jan 28;6:149. Available from: <URL>.

66. Thiyagu C, Manjubala I, Narendrakumar U. Thermal and morphological study of graphene based polyurethane composites. Mater Today Proc [Internet]. 2021;45:3982–5. Available from: <URL>.

67. Verma M, Chauhan SS, Dhawan SK, Choudhary V. Graphene nanoplatelets / carbon nano-tubes/polyurethane composites as efficient

shield against electromagnetic polluting radiations. Compos Part B Eng [Internet]. 2017 Jul 1;120:118–27. Available from: <URL>.

68. Gedam SS, Chaudhary AK, Vijayakumar RP, Goswami AK, Bajad GS, Pal D. Thermal, mechanical and morphological study of carbon nanotubes-graphene oxide and silver nanoparticles based polyurethane composites. Mater Res Express [Internet]. 2019 May 10;6(8):085308. Available from: <URL>.

69. Surekha G, Krishnaiah KV, Ravi N, Padma Suvarna R. FTIR, Raman and XRD analysis of graphene oxide films prepared by modified Hummers method. J Phys Conf Ser [Internet]. 2020 Mar 1 [cited 2023 Jun 22];1495(1):012012. Available from: <URL>.

70. Rao S, Upadhyay J, Polychronopoulou K, Umer R, Das R. Reduced Graphene Oxide: Effect of Reduction on Electrical Conductivity. J Compos Sci [Internet]. 2018 Apr 9;2(2):25. Available from: <URL>.

71. Khan QA, Shaur A, Khan TA, Joya YF, Awan MS. Characterization of reduced graphene oxide produced through a modified Hoffman method. Suvarapu LN, editor. Cogent Chem [Internet]. 2017 Jan 1;3(1):1298980. Available from: <URL>.

72. Romero A, Lavin-Lopez MP, Sanchez-Silva L, Valverde JL, Paton-Carrero A. Comparative study of different scalable routes to synthesize graphene oxide and reduced graphene oxide. Mater Chem Phys [Internet]. 2018 Jan 1;203:284–92. Available from: <URL>.

73. He J, Fang L. Controllable synthesis of reduced graphene oxide. Curr Appl Phys [Internet]. 2016 Sep 1;16(9):1152–8. Available from: <URL>.

74. Borand G, Akçamlı N, Uzunsoy D. Structural characterization of graphene nanostructures produced via arc discharge method. Ceram Int [Internet]. 2021 Mar 15;47(6):8044–52. Available from: <URL>.

75. Wang C, Song M, Chen X, Li D, Xia W, Xia W. Effects of Buffer Gases on Graphene Flakes Synthesis in Thermal Plasma Process at Atmospheric Pressure. Nanomaterials [Internet]. 2020 Feb 11;10(2):309. Available from: <URL>.

76. Muniyalakshmi M, Sethuraman K, Silambarasan D. Synthesis and characterization of graphene oxide nanosheets. Mater Today Proc [Internet]. 2020 Jan 1;21:408–10. Available from: <URL>.

77. Wan W, Zhao Z, Hu H, Gogotsi Y, Qiu J. Highly controllable and green reduction of graphene oxide to flexible graphene film with high strength. Mater Res Bull [Internet]. 2013 Nov 1;48(11):4797–803. Available from: <URL>.

78. AL-Saedi SI, Haider AJ, Naje AN, Bassil N. Improvement of Li-ion batteries energy storage by graphene additive. Energy Reports [Internet]. 2020 Feb 1;6:64–71. Available from: <URL>.

79. Johra FT, Lee J-W, Jung W-G. Facile and safe graphene preparation on solution based platform. J Ind Eng Chem [Internet]. 2014 Sep 25;20(5):2883–7. Available from: <URL>.

80. Tuinstra F, Koenig JL. Raman Spectrum of Graphite. J Chem Phys [Internet]. 1970 Aug 1;53(3):1126–30. Available from: <URL>.

81. Schönfelder R, Rümmeli MH, Gruner W, Löffler M, Acker J, Hoffmann V, et al. Purification-induced sidewall functionalization of magnetically pure single-walled carbon nanotubes. Nanotechnology [Internet]. 2007 Sep 19;18(37):375601. Available from: <URL>.

82. Herranz D, Muñoz-Martin M, Cañamero M, Mulero F, Martinez-Pastor B, Fernandez-Capetillo O, et al. Sirt1 improves healthy ageing and protects from metabolic syndrome-associated cancer. Nat Commun [Internet]. 2010 Apr 12;1(1):3. Available from: <URL>.

83. Wang H, Robinson JT, Li X, Dai H. Solvothermal Reduction of Chemically Exfoliated Graphene Sheets. J Am Chem Soc [Internet]. 2009 Jul 29;131(29):9910–1. Available from: <URL>.

84. Scardaci V, Compagnini G. Raman spectroscopy data related to the laser induced reduction of graphene oxide. Data Br [Internet]. 2021 Oct 1;38:107306. Available from: <URL>.

85. Scardaci V, Compagnini G. Raman Spectroscopy Investigation of Graphene Oxide Reduction by Laser Scribing. J Carbon Res [Internet]. 2021 Jun 17;7(2):48. Available from: <URL>.

86. Ferrari AC, Robertson J. Interpretation of Raman spectra of disordered and amorphous carbon. Phys Rev B [Internet]. 2000 May 15;61(20):14095. Available from: <URL>.

87. Hanifah MFR, Jaafar J, Aziz M, Ismail AF, A. Rahman M, Othman MHD. Synthesis of Graphene Oxide Nanosheets via Modified Hummers' Method and Its Physicochemical Properties. J Teknol [Internet]. 2015 Apr 15;74(1):189–92. Available from: <URL>.

88. Aliyev E, Filiz V, Khan MM, Lee YJ, Abetz C, Abetz V. Structural Characterization of Graphene Oxide: Surface Functional Groups and Fractionated Oxidative Debris. Nanomaterials [Internet]. 2019 Aug 18;9(8):1180. Available from: <URL>.

89. Stankovich S, Dikin DA, Piner RD, Kohlhaas KA, Kleinhammes A, Jia Y, et al. Synthesis of graphene-based nanosheets via chemical reduction of exfoliated graphite oxide. Carbon N Y [Internet]. 2007 Jun 1;45(7):1558–65. Available from: <URL>.

90. Zenkel C, Albuerne J, Emmler T, Boschetti-de-Fierro A, Helbig J, Abetz V. New strategies for the chemical characterization of multi-walled carbon nanotubes and their derivatives. Microchim Acta [Internet]. 2012 Oct 12;179(1–2):41–8. Available from: <URL>.

91. Cançado LG, Jorio A, Ferreira EHM, Stavale F, Achete CA, Capaz RB, et al. Quantifying Defects in Graphene via Raman Spectroscopy at Different

Excitation Energies. Nano Lett [Internet]. 2011 Aug 10;11(8):3190–6. Available from: <URL>.

92. Zhang Y, Tang T-T, Girit C, Hao Z, Martin MC, Zettl A, et al. Direct observation of a widely tunable bandgap in bilayer graphene. Nature [Internet]. 2009 Jun 11;459(7248):820–3. Available from: <URL>.

93. Fang W, Hsu AL, Caudillo R, Song Y, Birdwell AG, Zakar E, et al. Rapid Identification of Stacking Orientation in Isotopically Labeled Chemical-Vapor Grown Bilayer Graphene by Raman Spectroscopy. Nano Lett [Internet]. 2013 Apr 10;13(4):1541–8. Available from: <URL>.

94. Grodecki K, Jozwik I, Baranowski JM, Teklinska D, Strupinski W. SEM and Raman analysis of graphene on SiC(0001). Micron [Internet]. 2016 Jan 1;80:20–3. Available from: <URL>.

95. Dehghanzad B, Razavi Aghjeh MK, Rafeie O, Tavakoli A, Jameie Oskooie A. Synthesis and characterization of graphene and functionalized graphene via chemical and thermal treatment methods. RSC Adv [Internet]. 2016;6(5):3578–85. Available from: <URL>.

96. Wojtoniszak M, Mijowska E. Controlled oxidation of graphite to graphene oxide with novel oxidants in a bulk scale. J Nanoparticle Res [Internet]. 2012 Nov 30;14(11):1248. Available from: <URL>.